Energy Conversion and Management 258 (2022) 115495

Contents lists available at ScienceDirect

Energy Conversion and Management

journal homepage: www.elsevier.com/locate/enconman

An improved kinetic modelling of woody biomass gasification in a downdraft reactor based on the pyrolysis gas evolution

Karim Rabea [a,b,*], Stavros Michailos [a], Muhammad Akram [a], Kevin J. Hughes [a], Derek Ingham [a], Mohamed Pourkashanian [a]

[a] Energy 2050, Department of Mechanical Engineering, Faculty of Engineering, The University of Sheffield, Sheffield S3 7RD, UK
[b] Mechanical Power Engineering Department, Faculty of Engineering, Tanta University, Tanta 31511, Egypt

ARTICLE INFO

Keywords:
Aspen plus modelling
Kinetic model
Pyrolysis gas evolution
Woody biomass
Downdraft gasifier
Aspen plus/MATLAB connection

ABSTRACT

Biomass gasification technology is evolving and more research through modelling alongside the experimental work needs to be performed. In the past, all the attention has been concentrated on the combustion and reduction stages to be the controlling reactions while the pyrolysis is modelled as an instantaneous process. In this study, a new enhanced model for the gasification process in the downdraft reactor is proposed with a more realistic representation of the pyrolysis stage as a temperature-dependent sequential release of gases. The evolution of the pyrolysis gas, followed by the combustion and reduction reactions, are kinetically controlled in the proposed model which is developed within the Aspen Plus software package. The simulation of the reactor temperature profile and the evolution of the pyrolysis gas is carried out in an integrated MATLAB and Aspen Plus model. The proposed model has been validated against experimental data obtained from the gasification of different woody biomass types and considering a range of scale reactor and power loads. The predicted results are in very good agreement with the experimental data, and therefore the model can be used with confidence to perform a sensitivity analysis to predict the performance of a gasifier at different load levels corresponding to the air flow rate range of 3–10 L/s. As the supplied air flow rate increases, the LHV decreases but the gas yield behaves conversely, and in turn the cold gas efficiency is maintained at a good level of energy conversion at $\geq$ 70%. Furthermore, the variation in the biomass moisture content, which is commonly in the range of 5–25 % has a significant effect on the gasification efficiency. Such that biomass that has a high moisture content substantially reduces the CO content and consequently the LHV of the produced gas. Hence, it is important to maintain the moisture content at the lowest level.

1. Introduction

Recently, the whole world is looking forward to mitigate the detrimental effects of utilizing traditional fossil fuels, which are very apparent and mainly driving the climate change. Therefore, the transition of the energy sector towards renewable supplies is a necessary approach. Biomass is, in principle, considered a low carbon energy source that apart from power, can also serve as feedstock for a range of value added products such as fuels and chemicals. In order to achieve a clean and flexible conversion of biomass, the gasification process is a preferred choice, where almost the whole biomass content is exploited to yield its energy in the form of a gas fuel called synthesis gas (syngas) [1]. During the gasification process, the biomass is thermally dried and decomposed in an autothermal regime where a fraction of the biomass is combusted to provide the necessary heat to self-sustain the entire process. A major endothermic subprocess in the gasification process is the pyrolysis where the biomass particles release the volatile content under the effect of heat. Another endothermic subprocess is the reduction where the combustion products are reduced by the hot charcoal to produce the syngas which is mainly CO, H_2, CH_4, CO_2 and N_2. However, the process is very sophisticated and the extent of these gases depends on many factors such as the biomass characteristics, the reactor design and the operating conditions [2]. Hence, an interesting approach to follow, alongside the experimental work, is the mathematical modelling of the process for a comprehensive investigation and optimization. The simulation can be carried out through computational fluid dynamics (CFD) (e.g. ANSYS) [3] or through process modelling software (e.g. Aspen Plus) [4]. Additionally, the Artificial Neural Network (ANN) modelling approach can be utilized as a process simulation, where its basis is to

* Corresponding author.
E-mail addresses: kelamawy1@sheffield.ac.uk, karim_rabea@f-eng.tanta.edu.eg (K. Rabea).

https://doi.org/10.1016/j.enconman.2022.115495
Received 28 January 2022; Received in revised form 10 March 2022; Accepted 11 March 2022
Available online 23 March 2022

Nomenclature

A	Pre-exponential factor
[C]	Concentration
ANN	Artificial neural network
CCE	Carbon conversion efficiency
CFD	Computational fluid dynamics
CGE	Cold gas efficiency
CHP	Combined heat and power
d.a.f	Dry ash free
E	Activation energy
ER	Equivalence ratio
FC	Fixed carbon
$H_{f,B}$	Enthalpy of formation for biomass
$h_{f,i}$	Enthalpy of formation of species i
h_{fg}	Latent heat of water
HHV	Higher heating value
h_i	Sensible enthalpy of species i
K	Rate constant
LHV	Lower heating value
M	Molecular weight
MC	Moisture content
n	Reaction order
OLE	Object linking and embedding
RCSTR	Continuous stirring tank reactor
RGibbs	Minimum Gibbs free energy reactor
RMSD	Root mean square deviation
RPlug	Plug flow reactor
T_o	Reference temperature
VM	Volatile matter
wt.%	Weight percent
x	Mole fraction
X	Conversion
y	Mass fraction
v_i	Moles of species i
$\dot{Q}$	Rate of heat loss
$\dot{m}$	Mass flow rate
stoich	Stoichiometric
β	Heating rate

build knowledge from experiments and manage it to predict the numerical results without going through the mathematical governing equations of the process [5]. Aspen Plus is packed with a huge database of the thermal, physical and chemical properties of an extensive set of compounds and equipped with a bank of operation blocks comprising reactors, pressure changers, heaters, etc. These operation blocks are connected through material, heat and/or work streams in order to form a process flow sheet, where the solution of the governing models of the blocks and components is achieved.

Gasification is a chemical reaction process and from this perspective there are two main approaches to follow in the modelling, i.e., the thermodynamic equilibrium and the kinetic modelling. About two thirds of the modelling studies are based on the equilibrium approach and the rest implies some kinetic governing equations [6]. Owing to its simplicity, the thermodynamic equilibrium is a very common approach to estimate the ultimate achievable component mole fractions of the producer gas. This approach estimates the exit compositions by minimizing the Gibbs free energy of the system at a specified pressure and temperature [7]. This assumes the full mixing of the reactants and an infinite residence time (hence it is not dependent on of the gasifier geometry) [8]. In addition, some of the equilibrium-based models and their limitations regarding the results and interpretations are discussed in the following section.

In Aspen Plus, it is very common to pursue this approach and mostly by the implementation of the RGibbs reactor after the decomposition of biomass in the RYield block according to the ultimate analysis. In some studies, the simulation of gasifying different feedstocks was conducted by employing a single RGibbs reactor to represent the combustion and the reduction stages of gasification [9,10] or to represent the three stages of gasification (pyrolysis, combustion and reduction) [11,12]. Whereas, in some other studies, two RGibbs reactors were used to model the reduction and the combustion stages while the decomposition in the RYield block represented the pyrolysis stage as performed by Chen et al. [13] and Begum et al. [14]. A very common approach to follow for narrowing the gap in the model validation is to apply the restricted equilibrium within the same RGibbs block for particular reactions to be calculated at modified temperatures other than the main equilibrium temperature [12,15–17]. Although equilibrium modelling with Aspen Plus is adopted by most of the researchers, there are some deviations in the results compared to the experimental data, which is basically because the equilibrium is not reached and the predictions need to be fitted by unrealistic assumptions such as the restricted equilibrium. Therefore, the kinetic modelling using Aspen Plus can be applied for more precise simulations of the gasification reactions, the hydrodynamics inside the reactor as well as any reactor geometrical limitations.

Kinetic-based simulation of biomass gasification to predict the syngas composition is based on the significance of the reaction rates within a definite residence time or volume. To implement the chemical reaction kinetics, Aspen Plus offers two main blocks, i.e., continuous stirring tank reactor (RCSTR) and plug flow reactor (RPLUG). Due to the perfect mixing basis of the RCSTR reactor, it is commonly utilized for the fluidized bed gasifiers [18], whereas the RPLUG reactor has the capability to handle the reaction kinetics while considering the residence time by referencing to the reactor dimensions (length and diameter) [19]. Therefore, it is important to take care when selecting the appropriate block for the case study of interest.

Nikoo and Mahinpey [20] proposed a semi-kinetic model developed in Aspen Plus for the steady state operation of the bubbling fluidized bed reactor. Four RCSTR reactor blocks were used together with a user-defined Fortran code to simulate the hydrodynamics and the heterogeneous chemical reactions in two sections, i.e., the bed and freeboard of the fluidized bed gasifier. The pyrolysis and the homogenous reactions of the gasification process were modelled by the RGibbs reactor. The predicted values of CO_2 and H_2 were underestimated, in spite of the considerable convergence of H_2 at temperatures higher than 800 ℃. Later, Pauls et al. [21] improved this model through the inclusion of temperature-dependent empirical equations for the pyrolysis products in addition to the consideration of tar but the predictions of CO_2 and CH_4 were of low accuracy. Puig-Gamero et al. [22] implemented the same empirical equations of the pyrolysis products along with two consecutive RPlug reactors to simulate the combustion and reduction zones of a pilot-scale bubbling fluidized bed gasifier. In the model of Damartzis et al. [18], the pyrolysis, in addition to the heterogenous char gasification reactions, were assumed to reach equilibrium and they were modelled by two RGibbs reactors. On the other hand, the homogeneous reactions, together with tar oxidation were rate controlled and implemented in a RCSTR reactor. A different approach was followed by Cao et al. [23], where the pyrolysis and partial combustion of volatiles were operated in a single RGibbs reactor, but the gasification reactions, along with the tar cracking were incorporated in a RCSTR reactor. The results obtained using this model were in agreement with the experimental data obtained from the literature, except for CO_2 and CO and especially at higher temperatures, namely greater than 790 ℃.

Given that the pyrolysis stage is quite complex, different approaches

were followed to simulate this stage. In the equilibrium models, most researches considered the pyrolysis as the decomposition of the biomass inside the RYield reactor into the conventional components represented by the carbon (C), H_2, O_2, N_2, S and H_2O based on the mass balance with the ultimate analysis of the biomass. Instead, others specify the fractions of the volatile components and char from the experimental data and feed them into the RYield reactor [24]. Alternatively, Adnan et al. [25] used an initial guess accompanied by the elemental balance to estimate the volatile components concentrations. A similar methodology was executed by Tungalag et al. [26] for each species in the form of chemical equations and controlled by the ultimate analysis after the initial assumption of the volatile components including tar. These procedures are an approximation but in the following step, the RGibbs reactor usually adjusts all the components based on the minimization of the Gibbs free energy. For the kinetic modelling, the common approach is to utilize the RGibbs reactor for the pyrolysis stage [18,20,27–29]. Otherwise, empirical correlations with a Fortran subroutine is integrated into the RYield block to determine the mass yield of each component of the pyrolyzed gas, including tar as followed by Abdelouahed et al. [30], Beheshti et al. [31] and Pauls et al. [21]. Also, the same methodology that was used in the equilibrium can be applied in the kinetic modelling by using a single step model such that the fractions of the pyrolysis products are calculated based on the atom balance along with relative fractions of the constituents as presented in the model of Dang et al. [32].

In this study, an improved kinetic model to simulate the gasification process within the downdraft gasifier using Aspen Plus and MATLAB is developed by considering a more realistic approach for the pyrolysis stage. For instance, based on the pyrolysis of large particle woody biomass under non-isothermal decomposition, the non-condensable gas components are not released instantaneously during pyrolysis. Rather, the CO_2 and CO are released at the early stages of the pyrolysis process followed by CH_4 and in the later stage (higher temperatures) H_2 is released. This sequence of gases leaving the biomass particle is known as the gas evolution and has been reported in multiple experimental pyrolysis studies under different heating rates, such as [33–38]. The proposed model integrates the kinetics of the pyrolysis gas evolution according to the temperature profile of the gasifier, where they are modelled in MATLAB and the results are transferred to Aspen Plus. Furthermore, unlike most of the models in Aspen, the proposed model considers the dimensions of the gasification reactor. The model also includes the simulation of the power generation unit that utilizes the produced gas for electricity generation.

2. Materials and methods

2.1. Biomass characteristics

Since the thermal decomposition of the biomass is affected by the biomass particle size as well as the heating conditions, the proposed model incorporates a detailed representation of the gasification process with an emphasis in the pyrolysis stage. The utilized relevant pyrolysis data [33,37] are of large biomass particles and processed under non-isothermal conditions. Therefore, in this study, we have selected woody biomass as the feedstock due to the availability of pyrolysis experimental studies of large wood particles and the sequential gas release during pyrolysis that depends on the temperature profile of the gasifier. The proximate and ultimate analyses of wood chips are shown in Table 1, where MC, VM, and FC represent the moisture content, volatile matter, and fixed carbon, respectively.

Table 1
Proximate and ultimate analyses of wood chips [33,39].

Proximate analysis (wt.%)				Ultimate analysis (wt.%, dry basis)			
MC	VM	FC	Ash	C	H	N	O
8.35	74.8	18.4	6.8	43.75	5.75	1.65	42.05

2.2. Model description

In the downdraft gasifier, the biomass moves through different temperature zones inside the reactor and the highest temperature is attained around the air entrance level. Initially, the biomass releases the moisture content and then starts to release the volatiles (condensable tar and non-condensable gas) as it progresses to the higher temperature zones. Meanwhile, the gasification reactions take place between the released gas species and the solid char (both homogeneous and heterogeneous reactions). The temperature profile and the release of the non-condensable gases, which is a function of the temperature, have been modelled in MATLAB. The MATLAB model is integrated into the Aspen Plus software to complete the gasification model, and the flow chart of the proposed modelling approach is presented in Fig. 1.

In the pyrolysis stage, the decomposition of the biomass particles is obtained from the study of Yan et al. [33] which includes the pyrolysis of large particles of wood chips under different heating rate conditions.

$$\text{woodchip}(CH_{1.64}O_{0.69}) \rightarrow 0.5\text{char} + 0.087H_2 + 0.1CO + 0.063CO_2 + 0.035CH_4 + 0.09\text{Tar} + 0.12H_2O \quad (1)$$

There are many models in the literature regarding pyrolysis that consider the released gas as a unit without considering the rate of evolution of the individual components. Limited research exists dealing with the kinetic representation of the sequential order of the non-condensable gases release as a function of temperature. The Single Reaction Model as presented in the study of Ghodke et al. [37] and Gupta et al. [38], which has been utilized herein, can provide an accurate representation of the gas evolution. The evolution kinetics of the non-condensable gases, namely CO_2, CO, CH_4 and H_2, are to be described based on the non-isothermal pyrolysis of large particle biomass feedstocks. Where, it is important to consider the sequential order of the gas release from the biomass particles as it moves inside the gasifier through different temperature zones. This means the main driving force of the gas release is the temperature regardless the releasing time. The Single Reaction Model, that has been presented by Ghodke et al. [37] and Gupta et al. [38] for the gas evolution is considered herein and can be expressed as follows:.

$$\frac{dx}{dt} = k(1-x)^n x = \frac{v_i}{v_i^*} \quad (2)$$

where x is the mole fraction of each gas that evolves with time and is represented by the current yield (v_i) relative to the ultimate attainable yield for each gas (v_i^*) and k is the rate constant. For the non *iso*-thermal conditions, the rate equation becomes:

$$\frac{dx}{dT} = \frac{A}{\beta}\exp\left(\frac{-E}{RT}\right)(1-x)^n \quad (3)$$

where A is the pre-exponential factor,β is the heating rate (dT/dt), E is the activation energy, and n is the reaction order. The kinetic parameters (presented in Table 2) for the evolution rate of the non-condensable gases are obtained from the study of Ghodke and Mandapati, which is based on the pyrolysis of large wood particle under a heating rate of 15 K/min [37]. As similar sequential order of gas release is observed under different heating rates, and specifically between 5 and 30 K/min [33,37], a heating rate of 15 K/min can be considered as a good representation of the gas evolution as a function of temperature.

Since the rate equation does not take a form that is embedded in Aspen Plus, MATLAB has been used to solve this equation with the built-in ode45 solver which is based on the Runge-Kutta 4th order method and the obtained results are supplied to the model in Aspen. A connection between the two programs is established through a COM server

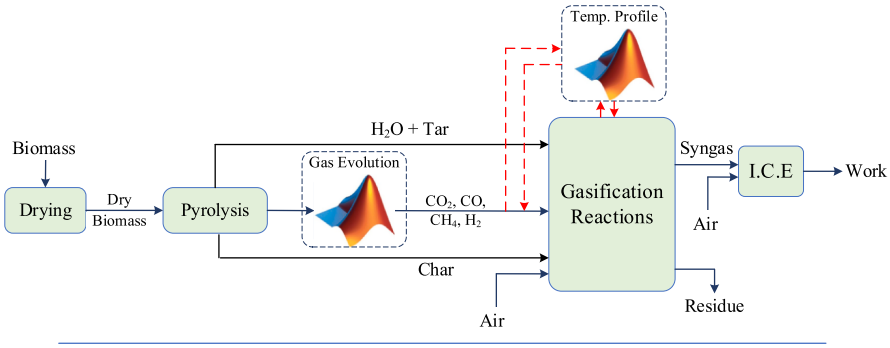

Fig. 1. The flow chart of the proposed modelling approach. The unit blocks have been modelled in Aspen Plus.

Table 2
Kinetic parameters for the pyrolysis gas evolution rate.

Gas Component	*E* (J/mole)	*A* (min^{-1})	Reaction order
CO_2	43,300	915.63	2
CO	37,810	33.75	2
CH_4	50,740	335.62	2
H_2	60,570	220.49	2

(actxserver) which creates a local OLE automation server with the program identification of Aspen as ('Apwn.Document.37.0').

Fig. 2 represents a plot of the solution of equation (3) for the non-condensable gases and depicts the sequence of the gas release from the biomass. For the combustion and reduction stages, the involved reactions, including the tar cracking, and their respective kinetic parameters are presented in Table 3.

2.3. Aspen plus model

The proposed model for the small-scale downdraft gasifier has been developed in the Aspen Plus simulation software. At first, the components that are included in the simulation are to be defined, while the biomass, char, and tar are introduced as non-conventional components due to their non-unique composition. Therefore, the biomass is recognized by substituting it with the conventional elements on the basis of

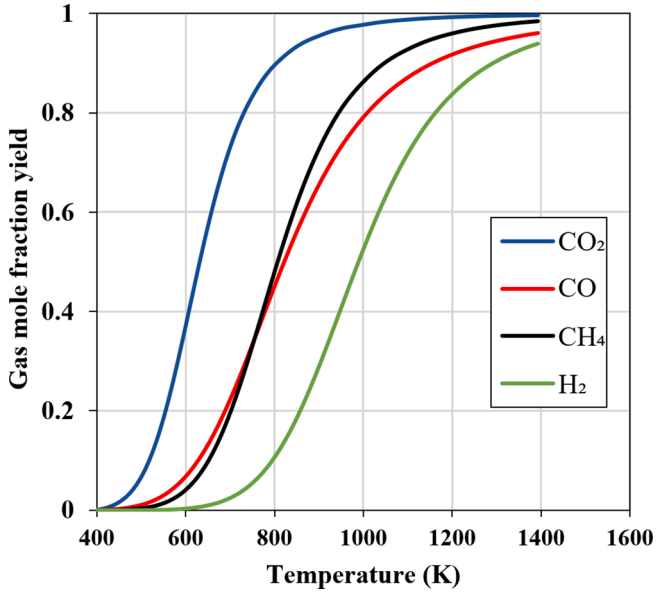

Fig. 2. Gas evolution as function of the temperature based on the heating rate of 15 K/min.

Table 3
Chemical reactions and kinetic parameters.

Reaction		Kinetic parameters		
		A (s^{-1})	E (J/mol)	Refs.
Combustion I	$C + 0.5O_2 \rightarrow CO$	$2.3T\times[O_2]^{0.4}$	92,300	[40]
Combustion II	$C + O_2 \rightarrow CO_2$	2512	53375.9	[41]
Boudouard	$C + CO_2 \rightarrow 2CO$	$4.4\ T \times[CO_2]^{0.6}$	162,000	[40]
Water gas reaction	$C + H_2O \rightarrow CO + H_2$	15,170	121,620	[42]
Methane formation	$C + 2H_2 \rightarrow CH_4$	4.189×10^{-3}	19,200	[43]
Combustion III	$CO + 0.5O_2 \rightarrow CO_2$	$1.3 \times 10^8[H_2O]^{0.5}[CO]^1[O_2]^{0.25}$	125,591	[44]
Water gas shift	$CO + H_2O \leftrightarrow CO_2 + H_2$	2780	12,560	[45]
	Reverse	95,862	46637.5	[45]
Methane reforming	$CH_4 + H_2O \leftrightarrow CO + 3H_2$	6.09×10^{14}	257,000	[46]
	Reverse	312	30,000	
Hydrogen combustion	$H_2 + 0.5O_2 \rightarrow H_2O$	2.2×10^9	109,000	[18]
Methane combustion	$CH_4 + 1.5O_2 \rightarrow CO + 2H_2O$	$5.0119 \times 10^{11}[CH_4]^{0.7}[O_2]^{0.8}$	202,504	[41]
Tar cracking	$Tar \rightarrow 0.3CO_2 + 2.43CO + H_2 + 0.67CH_4$	2.08×10^3	66,300	[47]

the ultimate analysis (C, H_2, O_2, N_2, S, Cl_2) [48]. The proximate and ultimate analyses are the main reference that enable the software to characterize the biomass using the built-in HCOALGEN and DCOALIGT models for the enthalpy and density, respectively. To calculate the properties of the included materials, the method of PR-BM is selected. In which, the equation of state follows the Peng-Robinson equation, while the thermodynamic properties follow the Boston Mathias Alpha function. This method is advised by the Aspen provider for the gas-based processes, and petrochemical applications.

The flow sheet of the gasification process followed by the power generation unit is shown in Fig. 3. Here the biomass stream is supplied under ambient conditions (25 °C and 1 atm) to the RYield block "DECOMP" to convert the biomass into conventional components, i.e., H_2O, C, H_2, N_2, CL_2 and O_2 based on the proximate and ultimate analyses of the biomass. The ash and N_2 are separated since they are considered as inert. Another RYield block "PYROL" is employed and supported by a FORTRAN calculator to simulate the primary pyrolysis stage, such that the mass yields of the primary pyrolysis products are defined on the basis of equation (1). From the equation of the tar cracking in Table 3 and the elemental balance, the ultimate analysis of the tar is obtained and defined in the same RYield block. The elemental composition of the char is defined as an export variable in the calculator "PYROL1" and

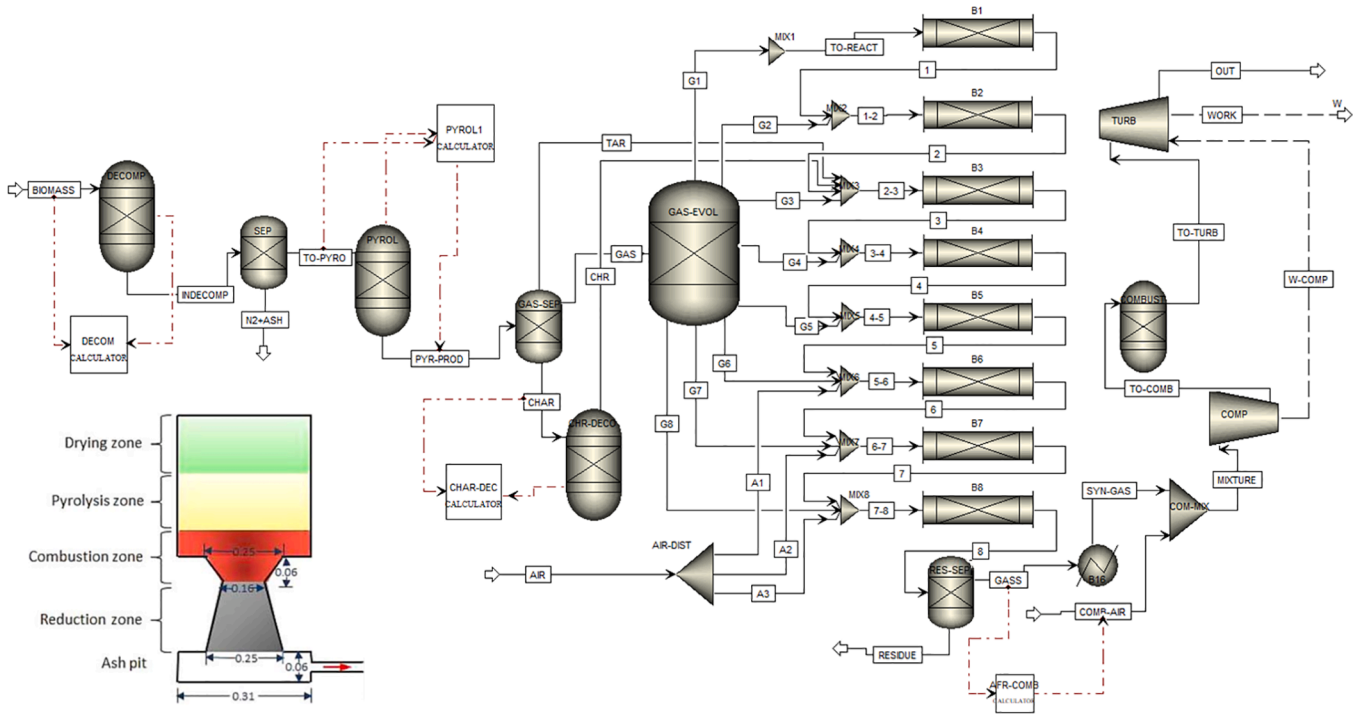

Fig. 3. Process flow diagram.

calculated as the remaining fractions of C, H, and O in the biomass according to equation (1). This char decomposes in the RYield block "CHR-DECO" at the temperature of 500 ℃ in the same way as the biomass decomposition in the early stage of the model. Subsequently, the values of the non-condensable gas components are split in the separator block "GAS-EVOL" before being introduced to the RPlug reactors to simulate the gasification reactions. Given that the biomass is pyrolyzed during its movement through the different temperature zones inside the gasifier, the non-condensable gases are not supplied in one batch. Instead, they are provided in 8 streams from G1 to G8 such that the first stream "G1" represents the initial release of the gases at a temperature up to 300 ℃, which is considered as the starting stage of the pyrolysis.

Similarly, the corresponding streams (G2 to G8) are assigned to the following stages of pyrolysis at temperatures related to the inlet temperature of each of the following RPlug reactors (B2 to B8). In order to specify the temperature of the RPlug reactors, a model is developed in MATLAB to simulate the temperature profile of the gasifier by applying the energy balance between the input material and the output of each section of interest (pyrolysis, combustion, and reduction). These sections are represented in the Aspen Plus model by the streams 5, 7, and 8, respectively (as depicted in Fig. 3). The temperature profile is for the axial direction (along the gasifier height), where the gasification reactions are taking place and the produced gas is generated while flowing through the gasifier bed in the axial direction. For the pyrolysis temperature (T_P), it is calculated using the following energy balance equation [49]:.

$$\dot{H}_{f,B}(T_o) = \sum_{i,out} \dot{m}_i \left[h_{f,i}(T_o) + h_i(T_p) - h_i(T_o) \right] + \dot{Q}_{pyr} \tag{4}$$

where, $h_i(T_p)$ is the enthalpy of the existing species (i) at T_p, $\dot{Q}_{pyr}$ is the heat necessary to achieve the biomass decomposition and $\dot{H}_{f,B}(T_o)$ is the enthalpy of formation of biomass at the reference temperature and can be calculated as follows:

$$\dot{H}_{f,B} = \dot{m}_B \left[(1 - \mathrm{MC}) \times h_{f,\mathrm{DB}}(T_o) + \mathrm{MC} \times h_{f,\mathrm{MC}}(T_o) \right] \tag{5}$$

Such that$\dot{m}_B$, $h_{f,DB}$ and $h_{f,MC}$ are the biomass flow rate and the enthalpies of formation of both the dry biomass and the moisture content (MC) in kJ/kg. Since the biomass varies in composition, its enthalpy of formation can be estimated based on its HHV and the stoichiometric combustion [7]_ENREF_7:.

$$h_{f,DB}(T_o) = HHV + \left[Y_C \times h_{f,CO2}(T_o) + 0.5 \times Y_H \times h_{f,H_2O}(T_o) \right] - \left[\left(A/F \right)_{stoic} \times h_{f,O_2}(T_o) \right] \tag{6}$$

where, the$(A/F)_{stoic}$, Y_C and Y_H are the stoichiometric air to fuel ratio and the mass fractions of carbon and hydrogen, respectively. This HHV (MJ/kg) can be calculated from the ultimate analysis and consequently the LHV (MJ/kg) is obtained by considering the latent heat of water (h_{fg}) from the hydrogen and moisture content as below [2,50]:

$$HHV_{biomass} = 0.3419\mathrm{C} + 1.1783\mathrm{H} + 0.1005\mathrm{S} - 0.1034\mathrm{O} - 0.015\mathrm{N} - 0.0211\mathrm{Ash} \tag{7}$$

$$\mathrm{LHV}_{biomass} = \mathrm{HHV} - h_{fg} \times (9Y_H + Y_{\mathrm{MC}}) \tag{8}$$

Based on Table 1, the calculated HHV and LHV for wood chips are 17.22 MJ/kg and 15.86 MJ/kg, respectively.

The pyrolysis heat is estimated as a function of the product of the LHV and the equivalence ratio (ER) along with the best approximation to the experimental results [42,49]. In the present model, it is considered to be 15% of that product, slightly higher than Diyoke et al. [49], to match the temperature profile of the small scale commercial downdraft gasifier operated by wood chips in the study of Ong et al. [39]. The equivalence ratio relates the actual air to fuel mass ratio and the stoichiometric one and can be expressed as follows:.

$$\mathrm{ER} = \frac{\left[\dot{m}_{air}/\dot{m}_B \right]_{actual}}{\left[\dot{m}_{air}/\dot{m}_B \right]_{stoich}} \tag{9}$$

where, the stoichiometric mass ratio can be calculated by the equation

below [51]:

$$\left[\frac{\dot{m}_{air}}{\dot{m}_{biomass}}\right]_{stoich} = \frac{1.293}{0.21}\left(1.866\frac{C_{daf}}{100} + 5.55\frac{H_{daf}}{100} + 0.7\frac{S_{daf}}{100} - 0.7\frac{O_{daf}}{100}\right) \quad (10)$$

such that the values of C_{daf}, H_{daf}, S_{daf} and O_{daf} represent the mass fractions of biomass elements on dry-ash-free basis (ultimate analysis, Table 1).

Similarly, the maximum temperature at the combustion zone as well as the final temperature at reduction zone, represented in Fig. 3 as streams 7 and 8, respectively, are calculated as follows:.

$$\dot{H}_{f,B} + \dot{H}_{f,air} = \sum_{i,out}\dot{m}_i\left[h_{f,i}(T_0) + h_i(T_{comb}) - h_i(T_o)\right] + \dot{Q}_{comb} \quad (11)$$

$$\dot{H}_{f,B} + \dot{H}_{f,air} = \sum_{i,out}\dot{m}_i\left[h_{f,i}(T_0) + h_i(T_{red}) - h_i(T_o)\right] + \dot{Q}_{red} \quad (12)$$

where, $\dot{Q}_{comb}$ and $\dot{Q}_{red}$ are the heat losses from the two zones and are estimated to be 11% and 35% of the product of LHV and ER, which are lower than that of Diyoke et al. [49]. The energy balance equations are solved in MATLAB where the connection with Aspen is useful to interchange the enthalpy of the streams and export the temperatures from MATLAB to Aspen Plus. The profiles of the temperature between the calculated points are assumed to be linear.

The RPlug reactor is a suitable choice to simulate the chemical reactions, as it can operate through a specific temperature profile along with a configuration of the geometry of the gasifier (diameter and height). The dimensions of the gasifier reactor are initially obtained from the small-scale commercial downdraft gasifier (GEK gasifier), a product of the company (All Power Labs), which has been operated in various studies, such as [33,36,39,52,53]23. The gasifier is a throated downdraft reactor with a height of 50 cm and a diameter of 31 cm at the drying zone, whereas the diameters at the throat section and at the end of reduction zone are 16 cm and 25 cm, respectively (see Fig. 3) and with a height difference of 25 cm above the grate. The gasifier height is divided equally with a step size of 5 cm for 7 blocks (B1 to B7) down to the throat (the highest temperature), while the reduction zone is simulated by the last RPlug reactor (B8). The 8 blocks of RPlug reactors are connected in sequential order such that the outlet stream of a block is directed and mixed with the pyrolysis gas then introduce to the following block. The extent of each component of the non-condensable gases in the split streams is determined from the solution of the rate equation (3) (presented in Fig. 2) with respect to the following RPlug inlet temperature. Such that, at the inlet of the last block (B8), all the remaining pyrolysis gases are supplied irrespective of the temperature. The air is supplied to the gasification reactors through a distributer "AIR-DIST" for the combustion reactions within the last three blocks (B6 to B8) to take into account the permeating air above and below the air entrance level. Since it is hard to be experimentally estimated, the split fractions of the air streams A1, A2 and A3 (as presented in Fig. 3) are fixed to 0.3, 0.5 and 0.2, respectively since these ratios achieve the optimum model predictions. The residual carbon and the water vapor in flow stream leaving the final reactor are separated in the block (RES-SEP), while the dry gas being directed to the power unit for electricity generation.

The 15 kWe power generation unit using internal combustion engine is simulated by a compressor, a RGibbs reactor, and a turbine, where the produced gas fuel is introduced along with the necessary air for complete combustion. The stoichiometric air is estimated in a calculator block "AFR-COMB" using the following equation:.

$$Air_{com}(kg/h) = 2.4514 \times CO + 34.32 \times H_2 + 17.16 \times CH_4 \quad (13)$$

where, Air_{com} is the mass flow rate of air in accordance with the mass flow rate of the combustible gas components (CO, H_2 and CH_4). As specified in the study of Maneerung et al. [52], the engine compression ratio is set to 10.25 for the compression stroke. The combustion of the compressed mixture is considered to take place under equilibrium conditions using the RGibbs reactor followed by the expansion through the turbine. The turbine output work is a representation of the electricity generated after subtracting the necessary compression work where a work stream (W-COMP) is connected.

2.4. Process evaluation parameters

It is important to estimate the heat content of the produced gas, expressed in the form of LHV, which can be estimated from the mole-based combustible gas constituents as follows [54]:.

$$LHV_{gas}\left(MJ/Nm^3\right) = \left[(10.79 \times H_2) + (12.636 \times CO) + (35.82 \times CH_4)\right] \quad (14)$$

In order to evaluate the energy conversion process, the cold gas efficiency (CGE) is the factor that relates the heat content of both the produced gas and the biomass. It can be calculated as follows [51]:.

$$CGE\% = \frac{V_{gas} \times [LHV]_{gas}}{\dot{m}_B \times [LHV]_{biomass}} \times 100\% \quad (15)$$

where, V_{gas} (Nm^3/h) is the rate of gas flow and $\dot{m}_B$ (kg/h) is the rate of biomass consumption, Another parameter to evaluate the continuous feeding operation is the carbon conversion efficiency (CCE), which expresses how much carbon is converted from the biomass to the gas as follows[51]:

$$CCE\% = \frac{12 \times (CO + CO_2 + CH_4)}{22.4 \times C} \times V_{gas} \times 100\% \quad (16)$$

where, C is the mass-based carbon content in the biomass.

3. Results and discussion

3.1. Model validation

Prior to discussing the model predictions in terms of the produced gas composition, it is important to validate the modelling of the gasifier temperature profile along its height, which affects the gasifier performance and outcomes. Thus, the predicted temperature profile is validated against relevant experimental data [39] at two different gasifier loads. At airflow rates of 4 L/s and 7 L/s, the calculated as well as the measured temperatures are presented in Fig. 4, where it can be seen that they are in a very good agreement. Notably, as expected, the increase in the airflow rate shifts the profile to higher temperatures. For instance, due to that increase in the airflow rate, the maximum temperature at the combustion zone has increased from 940 ℃ to 995 ℃ and at the end of the reduction zone an increase from 670 ℃ to 720 ℃ is observed.

In order to further evaluate the accuracy of the proposed gasification model, the predicted producer gas composition is compared with experimental results derived from Ong et al. [39]. In addition, the proposed model has been also compared with a 3D CFD kinetic model developed by Yan et al. [33], which simulates the axial and radial profile of the temperature and gas concentrations. Both studies [33 39] are based on the same biomass and the same gasifier design as the one that has been used in the present study. Fig. 5 shows that, in general, the proposed model prediction is accurate for all the gas components when compared to the experimental data as well as the other kinetic model. The prediction of H_2 from both models is in very good agreement with minor deviations, while an obvious improvement, compared to Yan's model [33], can be observed for the CH_4 and CO predictions.

However, the CO prediction is still overestimated and the CO_2 prediction is slightly underestimated compared to the experimental values. This slight mismatch can be considered as a limitation of the model, but the results are still in the good range with relative differences of 8.29% and 8.71% for CO and CO_2, respectively. Interestingly, the prediction of

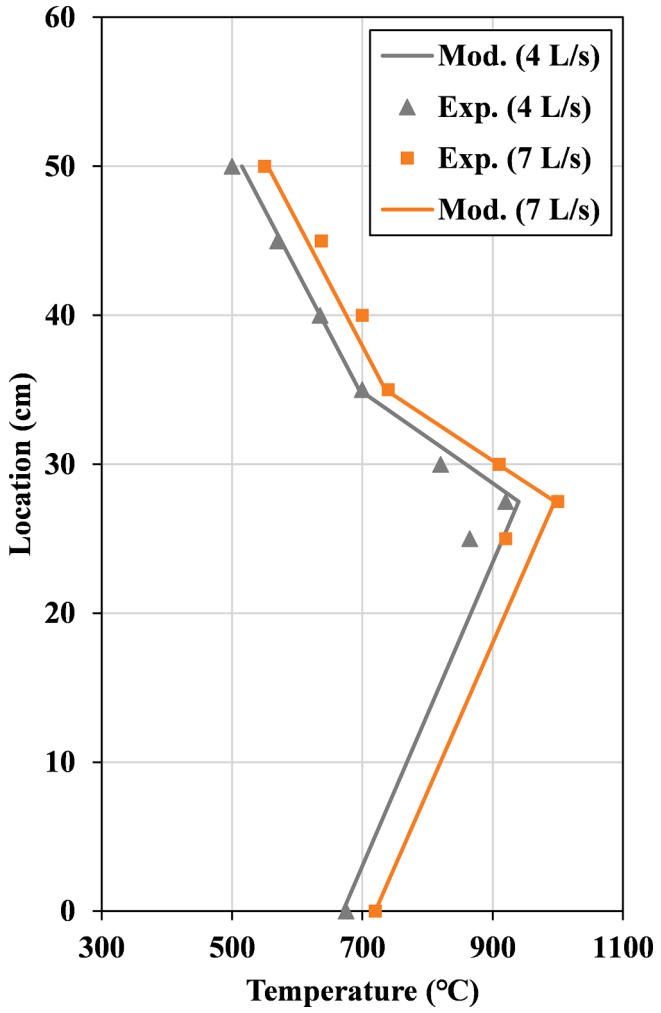

Fig. 4. Predicted and measured temperature profiles at the airflow rates of 4 L/s and 7 L/s [39].

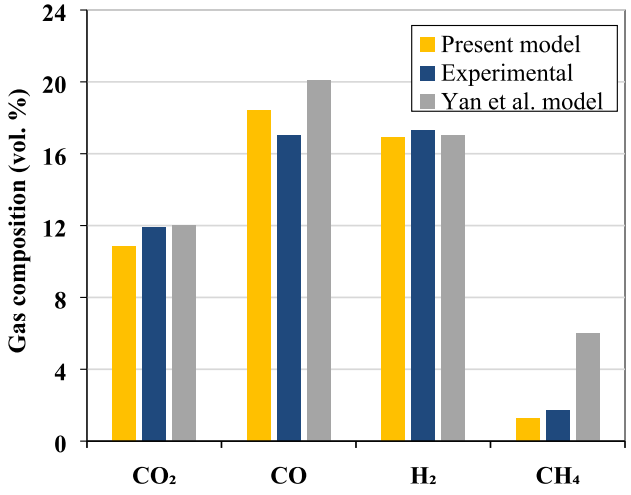

Fig. 5. Comparison of the predicted gas composition from the proposed model and from the Yan et al. [33] model against the experimental results of Ong et al. [39] at the airflow rate of 7 L/s and biomass flow rate of 16.2 kg/h.

CH_4 is improved significantly, where the relative difference between the experiment and the proposed model is 25.7% compared to 253% for the Yan et al. model [33]. The root-mean-square deviation (RMSD) is utilized to quantitatively evaluate the combined differences between the models and the experimental data by considering all the gas components, and it is calculated as follows:.

$$\mathrm{RMSD(vol\%)} = \sqrt{\frac{\sum_{i=1}^{n}(X_{i,exp} - X_{i,sim})^2}{n}} \quad (17)$$

where X_i is the mole fractions of the produced gas components from the experimental and the simulation results. The RMSD between the results of the proposed model and the experiment [39] is 0.825 vol%., while for the Yan et al. model [33], the RMSD is 2.626 vol%. Furthermore, when compared to other equilibrium and kinetic models of wood gasification from the literature, the RMSD was 2.532 vol% for the equilibrium model of Tauqir et al. [55] and 1.86 vol% for the kinetic model of Beheshti et al. [31].

In addition, the validation of the proposed model is carried out for other operating conditions, i.e., different power loads. For instance, at lower needs of power from the same gasifier, the air flow rate and consequently the biomass consumption rate are to be reduced and vice versa. From the same study of Ong et al. [39], at an air flow rate of 4 L/s and biomass feeding rate of 10 kg/h, the model results are presented. As depicted in Fig. 6, the model results are in a very good agreement with the experimental results and even improved for the CO_2, H_2, and CH_4 predictions with relative differences of 3.09%, 1.57%, and 6.2%, respectively. Whereas, a slight deviation is still detected for CO with a relative difference of 7.97%, but the RMSD for this case is better at 0.7065 vol%.

Furthermore, the proposed kinetic model is validated against the experimental data from the study of Shen et al. [36], which utilizes the same gasifier with a different type of biomass at an even lower load level. In addition, the biomass is wood pellets instead of wood chips and operated at an airflow rate of 3 L/s. The ultimate analysis of the wood pellets is very close to that of the woodchips as shown in Table 4. As we can see in Fig. 7, the accuracy of the prediction is high for the CO, and H_2 contents, whereas for CO_2 and CH_4, they deviate from the experimental results with relative differences of 28.8% and 29.7%, respectively. However, the overall RMSD is still good and at a value of 1.64 vol%.

Moreover, the validation of the model is reinforced by applying the model on other gasifier designs and using other woody biomass feedstocks. Hence, the proposed model is configured to the dimensions of the downdraft gasifier that is presented in the study of Machin et al. [56], which treats three different woody biomass types (Pine, Olive, and Peach). This gasifier has an internal diameter of 60 cm at the drying-pyrolysis zone, a throat of 25 cm in diameter and 38 cm in length, and

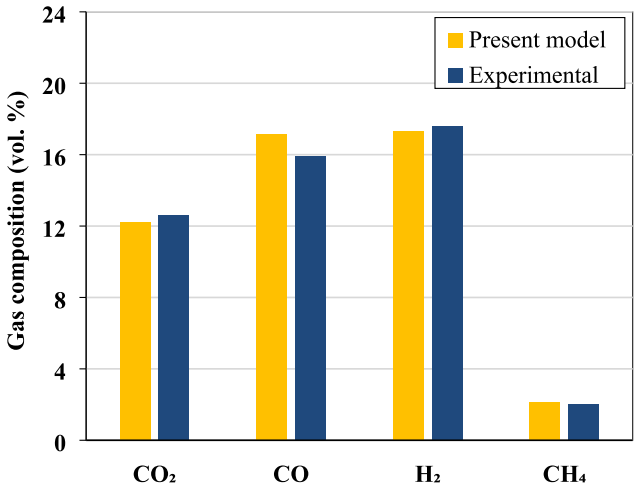

Fig. 6. Comparison of the syngas composition from the model and the experimental study [39] at the airflow rate of 4 L/s and biomass flow rate of 10 kg/h.

Table 4
Proximate and ultimate analyses of different woody biomass feedstocks.

Parameter	Wood pellets [36]	Pine [56]	Olive [56]	Peach [56]	Rubber wood [57]
Proximate analysis (wt.% dry basis)					
Moisture content (MC)	6.3	9	10.6	9.8	12.5
Volatile matters (VM)	82.5	n-a*	n-a	n-a	80.1
Fixed carbon (FC)	15.9	n-a	n-a	n-a	19.2
Ash	1.6	2.07	2.48	1.53	0.7
Ultimate analysis (wt.%, dry basis)					
Carbon	47.26	48.18	46.43	48.06	50.6
Hydrogen	6.14	5.71	5.63	5.83	6.5
Nitrogen	0.11	0.15	0.55	0.55	0.2
Sulfur	0	0	0	0	0
Oxygen	44.99	43.89	44.91	44.03	42
Properties					
HHV (MJ/kg) (Calculated)	18.71	18.13	17.8	18.71	20.6

*n-a: not available

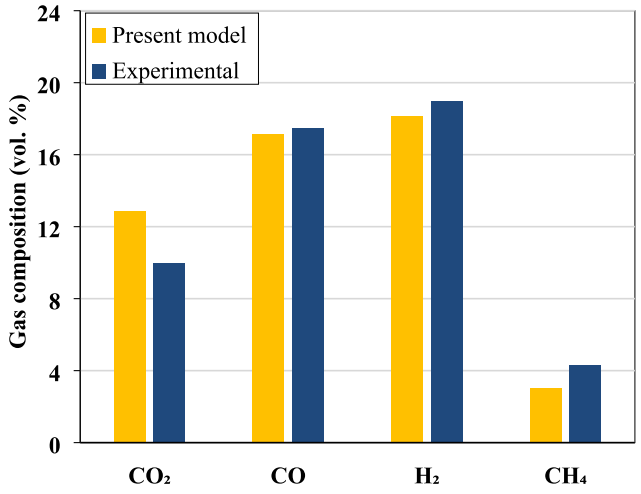

Fig. 7. Comparison between the predicted gas composition from the proposed model and the experimental results from Shen et al. [36] for wood pellets at an airflow rate of 3 L/s and biomass flow rate of 7.9 kg/h.

the reduction zone ends with a 50 cm diameter. In addition, the geometry of the downdraft gasifier of Jayah et al. [57] is considered for validation, whose results have been commonly used for validation in previous gasification model studies [10,49,58–61]8. This gasifier treats rubber wood, the throat diameter is 10 cm and the diameter at the end of reduction zone is 34 cm with a height difference of 22 cm [57]. The ultimate and proximate analyses of these woody biomass feedstocks are shown in Table 4. Since the values of VM and FC for Pine, Olive, and Peach biomasses were not available in the experimental study of Machin et al. [56], they have been denoted as not available. It is worth mentioning that, the most important data in our calculation is the elemental composition of the biomass.

The comparison between the model results and the experimental data is presented in Table 5. Generally, the model exhibits a reliable performance and relatively high accuracy with considerable low values of RMSD (between 1.757 and 1.178 vol%) for the different biomass types. For the design geometry of Machin et al. [56], the model overall results are in good agreement with the experimental data and the highest detected deviations are for the H_2 predictions, which are overestimated but within acceptable margins, i.e. 14.87%, 19%, and 9.93% for pine, olive, and peach, respectively.

For the case of the rubber wood in the gasifier of Jayah et al. [57], the model shows a very good accuracy of the syngas prediction with the low value of RMSD at 1.178 vol% to indicate this. In particular high accuracies have been observed for the CO_2, H_2 and CH_4 whereas the CO prediction is slightly underestimated by a relative difference of 12.4%.

3.2. Effect of the airflow rate on the gasification process

Many research studies in the literature, especially the modelling ones, have considered the effect of ER as a controllable input parameter through the change in the air (oxidizer) flow rate with the biomass feeding rate being constant. This independency between the air and the biomass feeding rates is not practical unless the solid residues disposal rate is considered, since the airflow rate is directly related to the biomass consumption rate [62]. Therefore, the more sensible approach for the steady state operation of the gasifier is to relate the biomass feeding rate to the airflow rate. To achieve that, based on the outcomes from the experimental studies including [63–68], the implication of a linear relationship between the flow rates of air and biomass has been found to be the best representation. By analysing these experimental data, this linear relationship is determined by setting an initial point from the case study [33,39] then investigating the effect of different gradients, bounded by the reported set of experimental air-biomass consumption data, to achieve the optimum validation against the experimental data of gas composition. As a result, the relation between the air mass flow rate and the biomass flow rate is governed by the equation: $\dot{m}_B = 0.482 * \dot{m}_{air} + 1.65$ as shown in Fig. 8.

In order to meet the variation in power load requirements, the main parameter to be changed is the airflow rate and therefore its effect on the produced gas composition is the main concern of any gasification process. Since, the extent of the main combustible components (CO, H_2 and CH_4) in the produced gas is the driving force of the following power generation process, Fig. 9 shows the predicted change in the gas components for the gasification of wood chips at different air flow rates. The model results along with the corresponding experimental data are shown to further support the reliability of the proposed model. As depicted, the model results show that the extent of CO_2 is declining from 12.2% to 9.93% and the CO is increasing from 17.18% to 19.4% with the increase in the airflow rate and these trends match the trends of the experimental data from Ong et al [39]. Since the temperature increases by the increase in the airflow rate, the endothermic reactions, such as the Boudouard reaction, takes more effect and in turn more C and CO_2 are converted to CO [69].

Table 5
Further evaluation of the model against more experimental data.

Biomass	Operating Conditions		CO_2	CO	H_2	CH_4	N_2	Ref.	RMSD (vol%)
Pine	Air = 1.5 L/s	Model	12.5	16.07	13.9	0.017	56.12		1.757
	$\dot{m}_B$ = 2.5 kg/h	Experiment	11.4	16	12.1	0.2	59.4	[56]	
Olive	Air = 1.6 L/s	Model	12.81	16.86	15.71	0.88	52.34		1.633
	$\dot{m}_B$ = 3.3 kg/h	Experiment	12.4	17.4	13.2	0.8	54.9	[56]	
Peach	Air = 1.47 L/s	Model	12.33	18.42	16.49	1.71	49.98		1.21
	$\dot{m}_B$ = 3.05 kg/h	Experiment	13.5	17.7	15	1.2	51.7	[56]	
Rubber wood	Air = 12.87 L/s	Model	9.99	16.73	12.83	1.27	56.9		1.178
	$\dot{m}_B$ = 20.9 kg/h	Experiment	10.7	19.1	13	1.2	56	[57]	

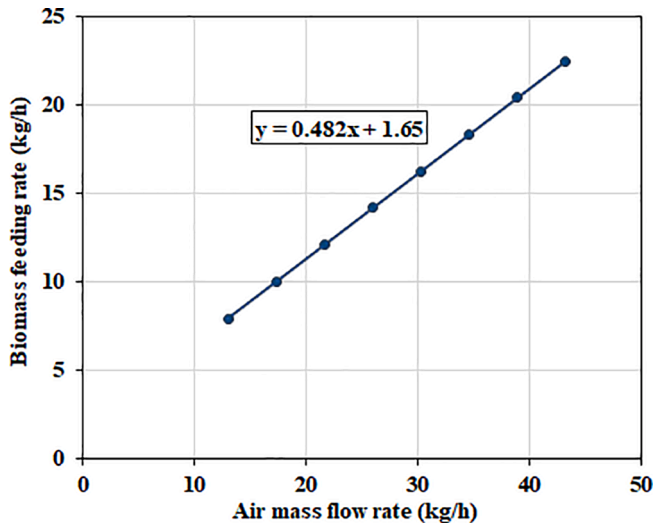

Fig. 8. The relation between the mass flow rates of air and biomass for wood chips gasification.

Given that the reverse water gas shift reaction is favored at high temperature, the extent of H_2 is slightly decreased. Also shown in Fig. 9, by the increase in the flowrate into the fixed geometry of the reactor, the CH_4 decreases from 2.12% to 0.7% and this is attributed to the slowness of the methane formation reaction [2]. The changes in the produced gas composition are directly exhibited as a change in the gas lower heating value (LHV) and consequently the gasification process efficiency. Although the apparent increase in the extent of CO, the LHV tends to decrease from 4.8 MJ/m^3 to 4.53 MJ/m^3 as shown in Fig. 10, and this is because of the decrease in CH_4, which has a much higher heating value compared to CO (see equation (14)). Interestingly, the cold gas efficiency shows an almost constant value at 71% (see Fig. 10), since the gas yield per unit mass of biomass consumed slightly increases and this effect offsets the decrease of LHV. This indicates that the wood chips gasification can operate for different power needs with a constant gasification process efficiency.

Furthermore, the model prediction for the effect of airflow rate on the residual mass, i.e., char and ash, which directly reflects the carbon conversion efficiency (CCE) is considered. Fig. 11 shows that by increasing the airflow rate from 4 L/s to 10 L/s, the residual mass relative to the biomass feeding rate decreases from 10.7% to 10.4%, which corresponds an increase of the CCE from 90.5% to 91.3%. Hence, the gasification process can exploit most of the wood chips, under different power loads.

In order to extend the parametric study of the effect of the airflow rate on a different type of woody biomass, it is reasonable to run the model using wood pellets, which is a standardized biomass and used in many studies in the literature. By building on the validation of the model for the wood pellets gasification at the airflow rate of 3 L/s (see Fig. 7), the effect of increasing the airflow rate up to 10 L/s on the gasifier outcomes is studied. Fig. 12 presents the trends of the syngas composition and it can be observed that these trends are similar to that of the wood chips gasification but with more declining trend of the H_2, i.e., from 18.2% to 14%. This can be attributed to the reverse water gas shift reaction, which is promoted by the higher operating temperature which in turn is a result of the higher energy content of the wood pellets compared to wood chips (18.71 MJ/kg vs 17.22 MJ/kg). In addition, the smaller moisture content of the wood pellets (6.3% compared to 8.35% of wood chips) further promotes the reverse water gas shift reaction and hence the H_2 consumption.

This apparent reduction in the concentration of H_2 and CH_4 by increasing the load directly reflects on the LHV of the syngas, which drops from 5.2 MJ/m^3 to 4.18 MJ/m^3 as shown in Fig. 13. These outcomes are in very good agreement with what has been observed for the gasification of another type of wood pellets using the same gasifier in the study of Maneerung et al. [52] when they increased the airflow rate from 3.67 L/s to 6.5 L/s. Also, Fig. 13 shows that the reduction in the LHV has been offset by an increase in the gas yield and consequently the CGE is not constant but even slightly increases from 70.6% to 73%, which is also in a good agreement with the experimental data from Maneerung et al. [52].

To estimate the extent of biomass conversion under different airflow

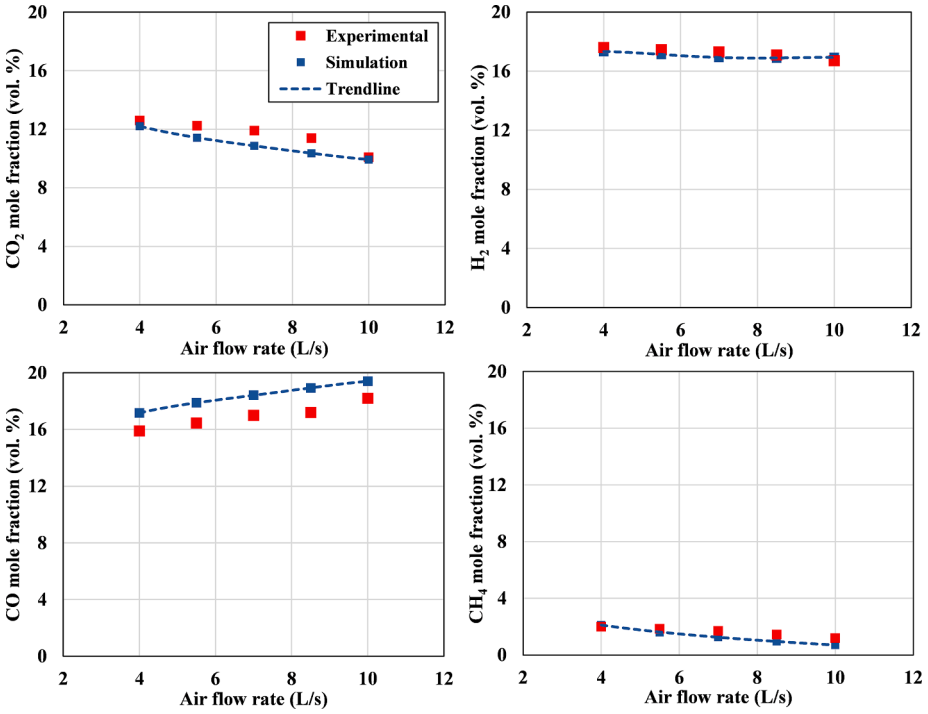

Fig. 9. Effect of the airflow rate on the syngas composition from the gasification of wood chips, simulation and experimental [39].

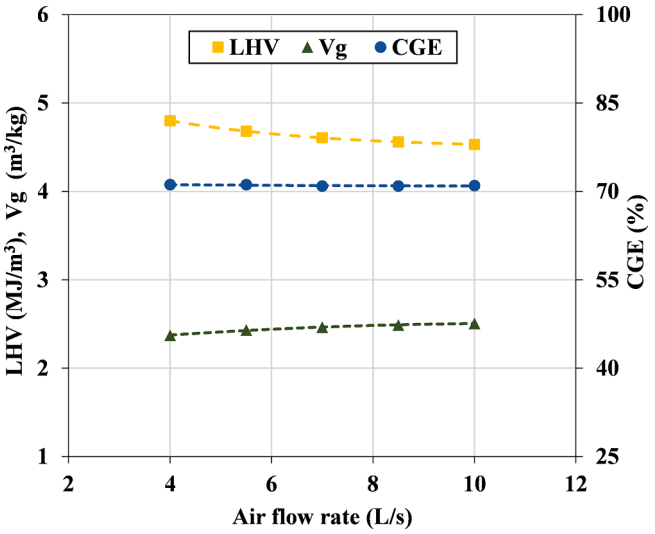

Fig. 10. Effect of the airflow rate on the gas LHV, gas yield (V_g) and CGE for wood chips gasification.

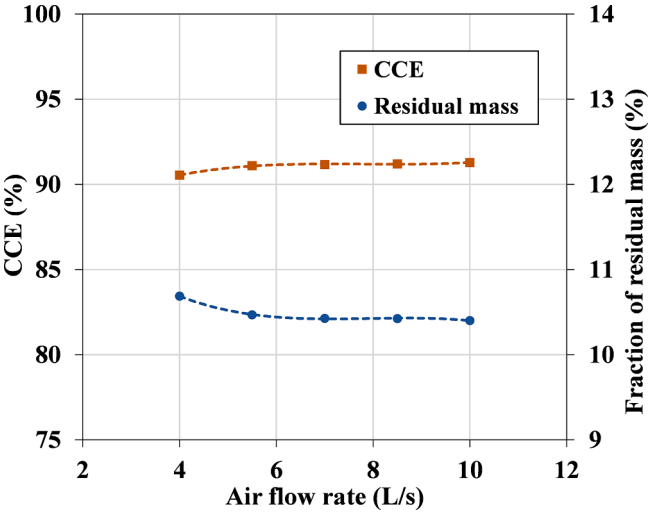

Fig. 11. Effect of the airflow rate on the residual mass fraction and the CCE for wood chips gasification.

rates, the fraction of the residual mass and the corresponding carbon conversion efficiency (CCE) are shown in Fig. 14. As depicted, the residual mass fraction declines significantly from 9% to 3.66% by increasing the airflow rate from 3 L/s to 10 L/s and in turn, the CCE increases from 84% to 96%. This diminution in the residual mass can be justified by the high heat content and the low moisture contents of the wood pellets. This assists in the boosting of the biomass conversion process under higher airflow rates, especially when accompanied by the availability of more carbon and less ash than that of the wood chips (see the ultimate analysis in Table 1 and Table 4).

Furthermore, for this model to be comprehensive, the prediction of the generated power based on the combustion engine is carried out at different airflow rates, which represents the controlling parameter and with wood chips and wood pellets as the feedstocks for the gasification. Fig. 15 reveals the range of operation for the integrated system of the gasifier and the power generation unit (15 kWe) at different levels of loading. By increasing the airflow rate from 3 L/s to 10 L/s, the attained power is increased from about 4.6 kW to 16.63 kW for the wood chips and to 15.35 kW for the wood pellets. The two biomass types can provide almost the same power at the light loads, while for the high-power

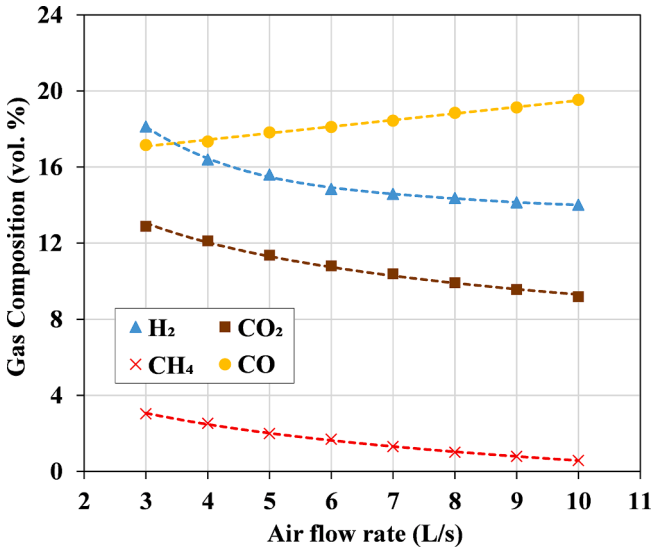

Fig. 12. Effect of the airflow rate on the syngas composition from the gasification of wood pellets.

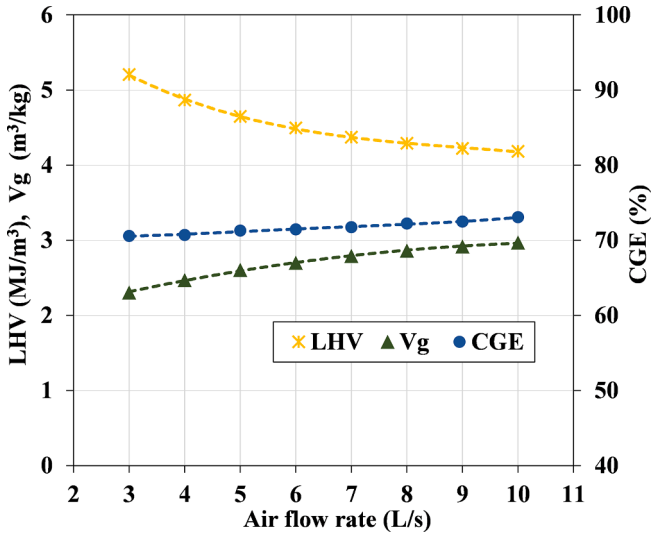

Fig. 13. Effect of the airflow rate on the LHV, gas yield, and CGE for wood pellets gasification.

needs, the wood pellets provides slightly lower power than the wood chips and this is due to the lower energy content in the produced gas from the gasifier at high airflow rates as illustrated in Fig. 13.

3.3. *Effect of the moisture content on the gasification process*

Another crucial parameter to be studied is the moisture content of the biomass and its impact on the gasification process. In this study, the moisture content is varied from 5% to 25%, and the other variables are kept constant. Based on the same gasifier geometry (GEK gasifier) and at the airflow rate of 7 L/s, the variation of the moisture content of two biomass types (wood chips and wood pellets) and its effect on the syngas composition as well as the process efficiency is investigated and presented in Fig. 16 and Fig. 17. The extent of the moisture content in the biomass has an obvious influence on the produced gas composition, especially the concentration of CO and consequently the CO_2, which essentially behave in a conflictive manner as shown in Fig. 16 (a) and Fig. 17 (a). The more moisture content in the biomass, the lower is the CO concentration, whereas the H_2 is almost constant to some extent and

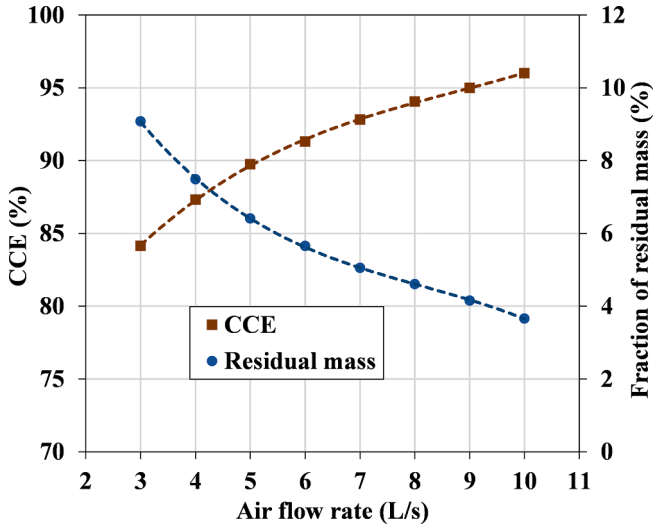

Fig. 14. Effect of the airflow rate on the residual mass fraction and the CCE for wood pellets gasification.

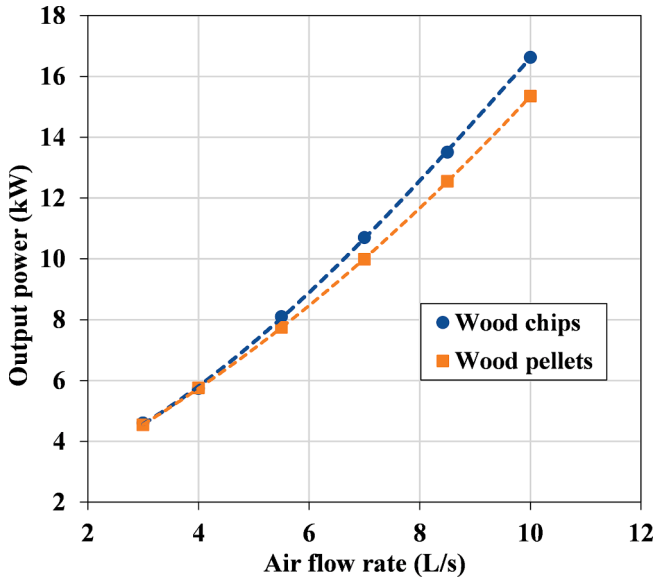

Fig. 15. Model prediction of the output power at different airflow rates for the wood chips and wood pellets gasification.

eventually decreases slightly at the higher levels of the moisture. The concentration of CH_4 has no significant change with the variation of the moisture content and hence, the change in CO represents the major drive to the gas LHV as well as the process efficiency indicators (CGE and CCE) as seen in Fig. 16 (b) and Fig. 17 (b). The mole fraction of CO declines from 19.8% to 12% for the wood chips and from 19.5% to 9.3% for the wood pellets, thus resulting in a reduction in the LHV from 4.7 MJ/m^3 to 3.78 MJ/m^3 and from 4.48 MJ/m^3 to 3.22 MJ/m^3, respectively. This trend in the gas concentrations matches very well the results obtained from previous studies [17,70] and this can be attributed to the reduction in the energy content of the biomass and accordingly the reduction of the temperature in the gasifier. Hence, the water gas shift reaction is favoured in the forward direction.

In an attempt to investigate the effect of the moisture content on the performance of a smaller scale gasifier, the geometry of the experimental investigation by Machin et al. [56] has been employed, against which the proposed model has been validated earlier in this study. The peach wood is the selected feedstock since it presents the lowest RMSD

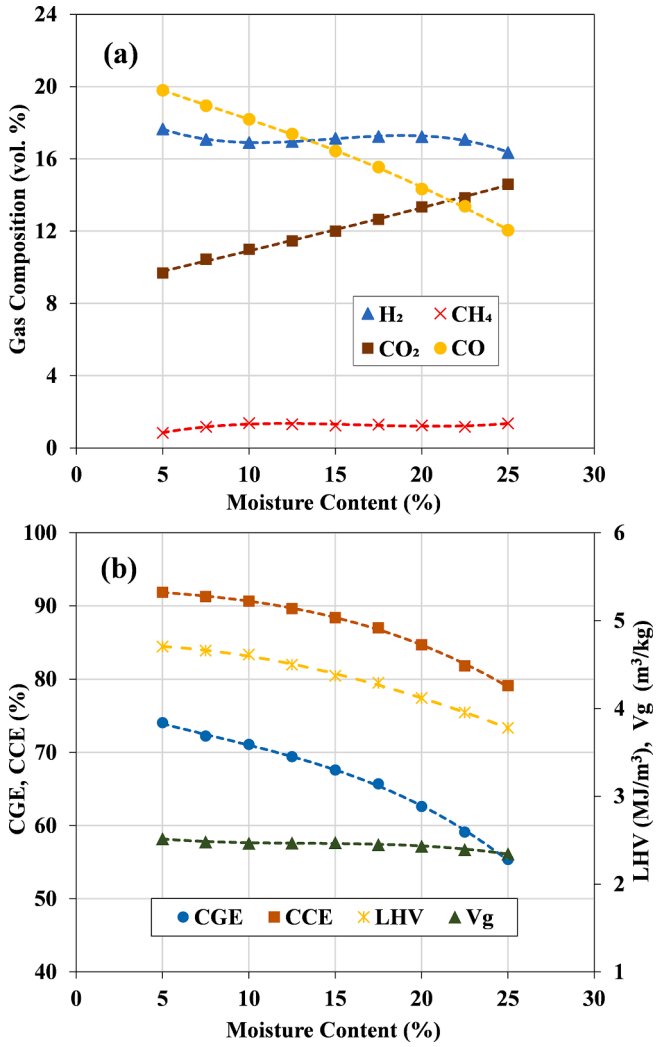

Fig. 16. Effect of the moisture content on (a): the syngas composition, (b): the gasification process efficiency for the wood chips gasification.

value between the experimental and the model results as depicted in Table 5. The sensitivity of the peach wood gasification to the moisture content is presented in Fig. 18, in which the change in the gas composition closely follows the same trend as the wood pellets with the larger gasifier. The dominant change is that for the CO concentration, which reduced from 21.4% to 11.45%, and accordingly the LHV and CGE reduced from 5.05 MJ/m^3 and 82.2% to 3.68 MJ/m^3 and 53.95%, respectively. The results indicate that the reduction rate of CO and the increase rate of CO_2 are slightly larger for the wood pellets and peach wood in comparison to the wood chips. This is because of the higher energy content of these biomass types and also this phenomenon can be observed in the results of Zainal et al. [71].

4. Conclusion

This study presents a new enhanced kinetic modelling approach for the gasification of woody biomass in a small-scale downdraft gasifier by introducing the pyrolysis gas components in a sequential order under the gas evolution kinetics. In addition, the combustion and reduction reactions of the gasification process are also rate-controlled to complete the proposed model. The model is built and operated in the Aspen Plus software along with an integrated connection with MATLAB which assists in overcoming the limitation of Aspen Plus in modelling the temperature profile and the gas evolution. The main outcomes of this study

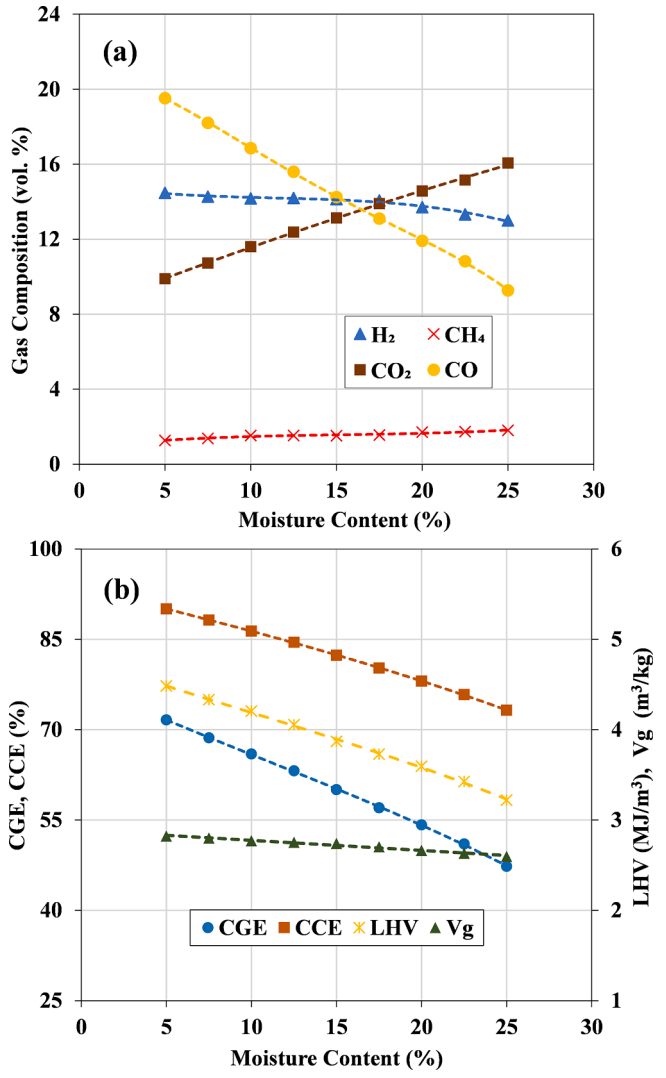

Fig. 17. Effect of the moisture content on (a): the syngas composition, (b): the gasification process efficiency for the wood pellets gasification.

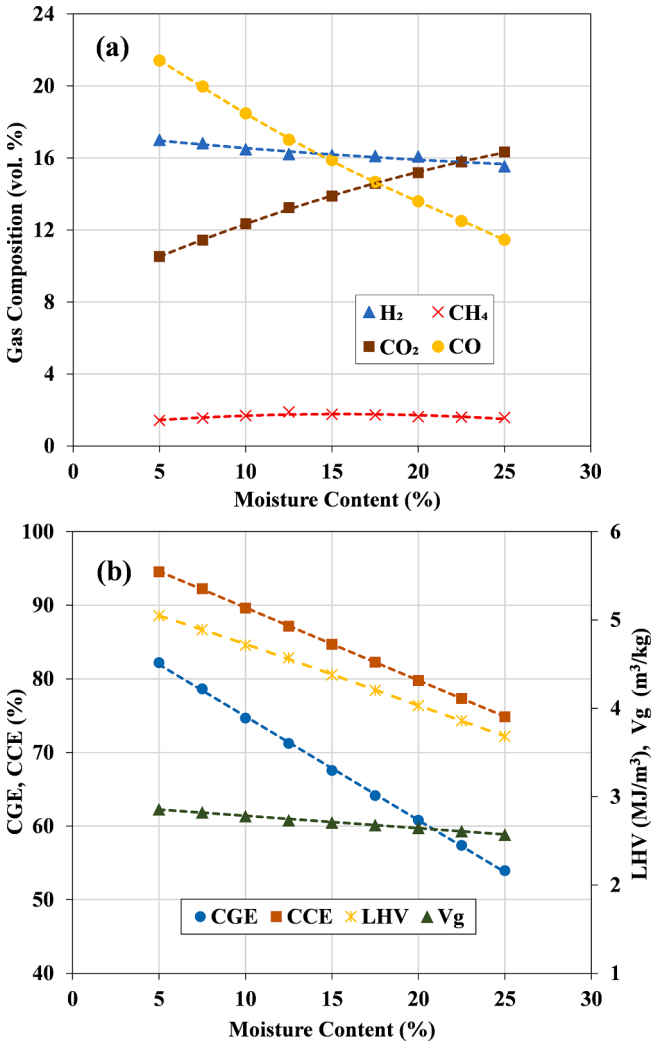

Fig. 18. Effect of the moisture content on (a): the syngas composition, (b): the gasification process efficiency for peach wood gasification.

can be summarized as follows:.

- When validating the proposed model against the experimental data for different woody biomass types, the model exhibited a very good capability of modelling the gasification process with the RMSD being in the range between 0.706 and 1.757 vol%.
- The model has been utilized to predict the performance of the gasifier at different power loads by increasing the airflow rate and was found that the CO content increased and the CO_2 and CH_4 decreased.
- The CGE is almost constant at 71% for the gasification of wood chips in spite of the increase in the airflow rate, where a slight increase is observed, and reaches 73% for the gasification of wood pellets. Hence, operation at different power loads for both biomass feedstocks appears to be efficient.
- On increasing the airflow rate from 3 L/s to 10 L/s boosts the conversion process and this is noticeable for the wood pellets, as the residual mass fraction of the biomass has decreased from 9% to 3.66% and in turn, the CCE has increased from 84% to 96%.
- At the low airflow rate of 3 L/s, the woodchips and wood pellets can provide a generated power of 4.6 kW, where a slightly growing gap arises, by increasing the airflow rate up to 10 L/s, between the two output power profiles in the favour of woodchips.
- The moisture content of the biomass showed a substantial effect on the performance of the gasifier irrespective of the scale and geometry. Whenever the moisture content is increased, the gasifier performance decreased significantly and the dominant change is noticed in the reduction of CO and the increase of CO_2, and accordingly in the decrease of the LHV and CGE. Therefore, the moisture content of the biomass is recommended to be at the lowest level prior to the gasification process.

The current study presented an enhanced approach to model the gasification process by including the pyrolysis gas evolution in a kinetic based model. The model has exhibited reliable predictions for the gasifier operation under different power loads. This variable load approach is beneficial for multiple gasification applications including power generation as well as chemicals and fuel production. Also, it can be very helpful in scale-up designs.

CRediT authorship contribution statement

Karim Rabea: Conceptualization, Formal analysis, Investigation, Methodology, Software, Validation, Writing – original draft. **Stavros Michailos:** Conceptualization, Methodology, Software, Validation, Writing – review & editing. **Muhammad Akram:** Methodology, Validation, Writing – review & editing. **Kevin J. Hughes:** Resources, Supervision, Writing – review & editing. **Derek Ingham:** Project

administration, Resources, Supervision, Writing – review & editing. **Mohamed Pourkashanian:** Resources, Supervision, Writing – review & editing.

Declaration of Competing Interest

The authors declare that they have no known competing financial interests or personal relationships that could have appeared to influence the work reported in this paper.

Acknowledgement

The first author acknowledges The Egyptian Ministry of Higher Education & Scientific Research and The British Council (Newton-Mosharafa Fund) for funding this research study at the University of Sheffield.

References

[1] Di Blasi C, Signorelli G, Portoricco G. Countercurrent fixed-bed gasification of biomass at laboratory scale. Ind Eng Chem Res 1999;38(7):2571–81.
[2] P. Basu, ''Biomass gasification, pyrolysis and torrefaction: practical design and theory''; 2013: Academic press.
[3] Janajreh I, Al Shrah M. Numerical and experimental investigation of downdraft gasification of wood chips. Energy Convers Manage 2013;65:783–92.
[4] Hantoko D, Yan M, Prabowo B, Susanto H, Li X, Chen C. Aspen Plus modeling approach in solid waste gasification. In: Current developments in biotechnology and bioengineering. Elsevier; 2019. p. 259–81.
[5] Puig-Arnavat M, Hernández JA, Bruno JC, Coronas A. Artificial neural network models for biomass gasification in fluidized bed gasifiers. Biomass Bioenergy 2013;49:279–89.
[6] Safarian S, Unnþórsson R, Richter C. A review of biomass gasification modelling. Renew Sustain Energy Rev 2019;110:378–91.
[7] S.R. Turns, ''INTRODUCTION TO COMBUSTION: Concepts and Applications''. 3rd ed ed. 2012: MCGRAW-HILL.
[8] Baruah D, Baruah D. Modeling of biomass gasification: A review. Renew Sustain Energy Rev 2014;39:806–15.
[9] Ramzan N, Ashraf A, Naveed S, Malik A. Simulation of hybrid biomass gasification using Aspen plus: A comparative performance analysis for food, municipal solid and poultry waste. Biomass Bioenergy 2011;35(9):3962–9.
[10] Tavares R, Monteiro E, Tabet F, Rouboa A. Numerical investigation of optimum operating conditions for syngas and hydrogen production from biomass gasification using Aspen Plus. Renewable Energy 2020;146:1309–14.
[11] Im-orb K, Simasatitkul L, Arpornwichanop A. Analysis of synthesis gas production with a flexible H2/CO ratio from rice straw gasification. Fuel 2016;164:361–73.
[12] Pala LPR, Wang Q, Kolb G, Hessel V. Steam gasification of biomass with subsequent syngas adjustment using shift reaction for syngas production: An Aspen Plus model. Renewable Energy 2017;101:484–92.
[13] Chen C, Jin Y-Q, Yan J-H, Chi Y. Simulation of municipal solid waste gasification in two different types of fixed bed reactors. Fuel 2013;103:58–63.
[14] Begum S, Rasul MG, Akbar D, Ramzan N. Performance analysis of an integrated fixed bed gasifier model for different biomass feedstocks. Energies 2013;6(12):6508–24.
[15] Kabir MJ, Chowdhury AA, Rasul MG. Pyrolysis of municipal green waste: a modelling, simulation and experimental analysis. Energies 2015;8(8):7522–41.
[16] Fernandez-Lopez M, Pedroche J, Valverde J, Sanchez-Silva L. Simulation of the gasification of animal wastes in a dual gasifier using Aspen Plus®. Energy Convers Manage 2017;140:211–7.
[17] Han J, Liang Y, Hu J, Qin L, Street J, Lu Y, et al. Modeling downdraft biomass gasification process by restricting chemical reaction equilibrium with Aspen Plus. Energy Convers Manage 2017;153:641–8.
[18] Damartzis T, Michailos S, Zabaniotou A. Energetic assessment of a combined heat and power integrated biomass gasification–internal combustion engine system by using Aspen Plus®. Fuel Process Technol 2012;95:37–44.
[19] Adeyemi I, Janajreh I. Modeling of the entrained flow gasification: Kinetics-based ASPEN Plus model. Renewable Energy 2015;82:77–84.
[20] Nikoo MB, Mahinpey N. Simulation of biomass gasification in fluidized bed reactor using ASPEN PLUS. Biomass Bioenergy 2008;32(12):1245–54.
[21] Pauls JH, Mahinpey N, Mostafavi E. Simulation of air-steam gasification of woody biomass in a bubbling fluidized bed using Aspen Plus: A comprehensive model including pyrolysis, hydrodynamics and tar production. Biomass Bioenergy 2016;95:157–66.
[22] Puig-Gamero M, Pio D, Tarelho L, Sánchez P, Sanchez-Silva L. Simulation of biomass gasification in bubbling fluidized bed reactor using aspen plus®. Energy Convers Manage 2021;235:113981.
[23] Cao Y, Wang Q, Du J, Chen J. Oxygen-enriched air gasification of biomass materials for high-quality syngas production. Energy Convers Manage 2019;199:111628.
[24] Tapasvi D, Kempegowda RS, Tran K-Q, Skreiberg Ø, Grønli M. A simulation study on the torrefied biomass gasification. Energy Convers Manage 2015;90:446–57.
[25] Adnan MA, Susanto H, Binous H, Muraza O, Hossain MM. Enhancement of hydrogen production in a modified moving bed downdraft gasifier–A thermodynamic study by including tar. Int J Hydrogen Energy 2017;42(16):10971–85.
[26] Tungalag A, Lee B, Yadav M, Akande O. Yield prediction of MSW gasification including minor species through ASPEN plus simulation. Energy 2020;198:117296.
[27] Begum S, Rasul MG, Akbar D, Cork D. An experimental and numerical investigation of fluidized bed gasification of solid waste. Energies 2014;7(1):43–61.
[28] Yu J, Smith JD. Validation and application of a kinetic model for biomass gasification simulation and optimization in updraft gasifiers. Chem Eng Process-Process Intensificat 2018;125:214–26.
[29] Smith JD, Alembath A, Al-Rubaye H, Yu J, Gao X, Golpour H. Validation and application of a kinetic model for downdraft biomass gasification simulation. Chem Eng Technol 2019;42(12):2505–19.
[30] Abdelouahed L, Authier O, Mauviel G, Corriou J-P, Verdier G, Dufour A. Detailed modeling of biomass gasification in dual fluidized bed reactors under Aspen Plus. Energy Fuels 2012;26(6):3840–55.
[31] Beheshti S, Ghassemi H, Shahsavan-Markadeh R. Process simulation of biomass gasification in a bubbling fluidized bed reactor. Energy Convers Manage 2015;94:345–52.
[32] Dang Q, Zhang X, Zhou Y, Jia X. Prediction and optimization of syngas production from a kinetic-based biomass gasification process model. Fuel Process Technol 2021;212:106604.
[33] Yan W-C, Shen Y, You S, Sim SH, Luo Z-H, Tong YW, et al. Model-based downdraft biomass gasifier operation and design for synthetic gas production. J Cleaner Prod 2018;178:476–93.
[34] Pattanotai T, Watanabe H, Okazaki K. Experimental investigation of intraparticle secondary reactions of tar during wood pyrolysis. Fuel 2013;104:468–75.
[35] Lestinsky P, Palit A. Wood pyrolysis using aspen plus simulation and industrially applicable model. GeoSci Eng 2016;62(1):11.
[36] Shen Y, Li X, Yao Z, Cui X, Wang C-H. CO2 gasification of woody biomass: Experimental study from a lab-scale reactor to a small-scale autothermal gasifier. Energy 2019;170:497–506.
[37] Ghodke P, Mandapati RN. Investigation of particle level kinetic modeling for babul wood pyrolysis. Fuel 2019;236:1008–17.
[38] Gupta A, Thengane SK, Mahajani S. Kinetics of pyrolysis and gasification of cotton stalk in the central parts of India. Fuel 2020;263:116752.
[39] Ong Z, Cheng Y, Maneerung T, Yao Z, Tong YW, Wang CH, et al. Co-gasification of woody biomass and sewage sludge in a fixed-bed downdraft gasifier. AIChE J 2015;61(8):2508–21.
[40] Kumar M, Ghoniem AF. Multiphysics simulations of entrained flow gasification. Part II: Constructing and validating the overall model. Energy Fuels 2012;26(1):464–79.
[41] Wu Y, Zhang Q, Yang W, Blasiak W. Two-dimensional computational fluid dynamics simulation of biomass gasification in a downdraft fixed-bed gasifier with highly preheated air and steam. Energy Fuels 2013;27(6):3274–82.
[42] Salem AM, Paul MC. An integrated kinetic model for downdraft gasifier based on a novel approach that optimises the reduction zone of gasifier. Biomass Bioenergy 2018;109:172–81.
[43] Wang Y, Kinoshita C. Kinetic model of biomass gasification. Sol Energy 1993;51(1):19–25.
[44] Sharma AK. Modeling and simulation of a downdraft biomass gasifier 1. Model development and validation. Energy Convers Manage 2011;52(2):1386–96.
[45] Gómez-Barea A, Leckner B. Modeling of biomass gasification in fluidized bed. Prog Energy Combust Sci 2010;36(4):444–509.
[46] Robinson PJ, Luyben WL. Simple dynamic gasifier model that runs in Aspen Dynamics. Ind Eng Chem Res 2008;47(20):7784–92.
[47] Cheng Y, Thow Z, Wang C-H. Biomass gasification with CO2 in a fluidized bed. Powder Technol 2016;296:87–101.
[48] Mutlu ÖÇ, Zeng T. Challenges and Opportunities of Modeling Biomass Gasification in Aspen Plus: A Review. Chem Eng Technol 2020;43(9):1674–89.
[49] Diyoke C, Gao N, Aneke M, Wang M, Wu C. Modelling of down-draft gasification of biomass–An integrated pyrolysis, combustion and reduction process. Appl Therm Eng 2018;142:444–56.
[50] Channiwala S, Parikh P. A unified correlation for estimating HHV of solid, liquid and gaseous fuels. Fuel 2002;81(8):1051–63.
[51] Guo F, Dong Y, Dong L, Guo C. Effect of design and operating parameters on the gasification process of biomass in a downdraft fixed bed: An experimental study. Int J Hydrogen Energy 2014;39(11):5625–33.
[52] Maneerung T, Li X, Li C, Dai Y, Wang C-H. Integrated downdraft gasification with power generation system and gasification bottom ash reutilization for clean waste-to-energy and resource recovery system. J Cleaner Prod 2018;188:69–79.
[53] Madadian E, Orsat V, Lefsrud M. Comparative study of temperature impact on air gasification of various types of biomass in a research-scale down-draft reactor. Energy Fuels 2017;31(4):4045–53.
[54] Striūgas N, Zakarauskas K, Džiugys A, Navakas R, Paulauskas R. An evaluation of performance of automatically operated multi-fuel downdraft gasifier for energy production. Appl Therm Eng 2014;73(1):1151–9.
[55] Tauqir W, Zubair M, Nazir H. Parametric analysis of a steady state equilibrium-based biomass gasification model for syngas and biochar production and heat generation. Energy Convers Manage 2019;199:111954.
[56] Machin EB, Pedroso DT, Proenza N, Silveira JL, Conti L, Braga LB, et al. Tar reduction in downdraft biomass gasifier using a primary method. Renewable Energy 2015;78:478–83.
[57] Jayah T, Aye L, Fuller RJ, Stewart D. Computer simulation of a downdraft wood gasifier for tea drying. Biomass Bioenergy 2003;25(4):459–69.
[58] Barman NS, Ghosh S, De S. Gasification of biomass in a fixed bed downdraft gasifier–A realistic model including tar. Bioresour Technol 2012;107:505–11.

[59] Sharma AK. Equilibrium and kinetic modeling of char reduction reactions in a downdraft biomass gasifier: A comparison. Sol Energy 2008;82(10):918–28.
[60] Boiger G, Buff V, Sharman D, Boldrini M, Lienhard V, Drew D. Simulation-based investigation of tar formation in after-treatment systems for biomass gasification. Biomass Convers Biorefin 2021;11(1):39–56.
[61] Jia J, Xu L, Abudula A, Sun B. Effects of operating parameters on performance of a downdraft gasifier in steady and transient state. Energy Convers Manage 2018;155:138–46.
[62] Upadhyay DS, Sakhiya AK, Panchal K, Patel AH, Patel RN. Effect of equivalence ratio on the performance of the downdraft gasifier–An experimental and modelling approach. Energy 2019;168:833–46.
[63] Rabea K, Bakry AI, Khalil A, El-Fakharany MK, Kadous M. Real-time performance investigation of a downdraft gasifier fueled by cotton stalks in a batch-mode operation. Fuel 2021;300:120976. https://doi.org/10.1016/j.fuel.2021.120976.
[64] Sharma S, Sheth PN. Air–steam biomass gasification: experiments, modeling and simulation. Energy Convers Manage 2016;110:307–18.
[65] Elder T, Groom LH. Pilot-scale gasification of woody biomass. Biomass Bioenergy 2011;35(8):3522–8.
[66] Hsi C-L, Wang T-Y, Tsai C-H, Chang C-Y, Liu C-H, Chang Y-C, et al. Characteristics of an air-blown fixed-bed downdraft biomass gasifier. Energy Fuels 2008;22(6):4196–205.
[67] Lv P, Yuan Z, Ma L, Wu C, Chen Y, Zhu J. Hydrogen-rich gas production from biomass air and oxygen/steam gasification in a downdraft gasifier. Renewable Energy 2007;32(13):2173–85.
[68] Sheth PN, Babu B. Production of hydrogen energy through biomass (waste wood) gasification. Int J Hydrogen Energy 2010;35(19):10803–10.
[69] Lv P, Xiong Z, Chang J, Wu C, Chen Y, Zhu J. An experimental study on biomass air–steam gasification in a fluidized bed. Bioresour Technol 2004;95(1):95–101.
[70] Antonopoulos I-S, Karagiannidis A, Gkouletsos A, Perkoulidis G. Modelling of a downdraft gasifier fed by agricultural residues. Waste Manage 2012;32(4):710–8.
[71] Zainal Z, Ali R, Lean C, Seetharamu K. Prediction of performance of a downdraft gasifier using equilibrium modeling for different biomass materials. Energy Convers Manage 2001;42(12):1499–515.